Double Photoionization of Spatially Aligned D_2

R. Dörner,[1,*] H. Bräuning,[2,3] O. Jagutzki,[1] V. Mergel,[1] M. Achler,[1] R. Moshammer,[1] J. M. Feagin,[4] T. Osipov,[2] A. Bräuning-Demian,[1] L. Spielberger,[1] J. H. McGuire,[1] M. H. Prior,[3] N. Berrah,[5] J. D. Bozek,[3] C. L. Cocke,[2] and H. Schmidt-Böcking[1]

[1]*Institut für Kernphysik, Universität Frankfurt, August Euler Strasse 6, D60486 Frankfurt, Germany*
[2]*Department of Physics, Kansas State University, Manhattan, Kansas 66506*
[3]*Lawrence Berkeley National Laboratory, Berkeley, California 94720*
[4]*Department of Physics, California State University-Fullerton, Fullerton, California 92834*
[5]*Department of Physics, Western Michigan University, Kalamazoo, Michigan 49008*

(Received 23 July 1998)

The four-body breakup of spatially aligned D_2 by 58.8 eV photons from the Advanced Light Source has been investigated by measuring the three dimensional momentum vectors of both fragment ions and one of the two electrons in coincidence. Energy and angular correlation between ions and electrons is discussed. We find rotational symmetry of the electron angular distribution around the polarization vector of the light and significant differences between helium and D_2 as well as between molecular alignment parallel and perpendicular to the polarization axis. [S0031-9007(98)08045-4]

PACS numbers: 33.80.Eh, 32.80.Fb

Ejection of both electrons from a bound two-electron system by a single photon is a remarkable consequence of electron-electron correlation. This subtle and fundamental process of double photoionization can be studied in the neutral two-electron systems helium and D_2 [1–3]. The complete fragmentation of D_2 provides a link between atomic and molecular photoionization studies. Here the initial state is a simple molecular system, and the final state is an unbound four-body Coulomb system with no molecular degrees of freedom. Unlike fragmentation of more complex molecules, where the photoejection of an electron is usually followed by molecular rearrangement which eventually leads to fragmentation, double photoionization of D_2 leaves two bare ions in a mutually repulsive Coulomb potential. Thus detection of the momentum vectors of the two outgoing nuclei provides a direct image of the spatial alignment of the two nuclear centers at the instant of double ionization [4,5].

In this work we have measured the direction and energy of the two ionic fragments in coincidence with the momentum vector of one of the two electrons from D_2 double ionization by linear polarized photons ($S_1 = 0.99 \pm 0.01$) at $E_\gamma = 58.8$ eV. At this energy, the two electrons share about 7 eV. This provides the connection between the ionic and the electronic motion in the continuum. It shows the direction in which one electron emerges from the molecule and how the available excess energy is shared between the nuclear fragments and the electrons. Our spectrometer has a 4π solid angle acceptance for ions and electrons. Thus we image the full momentum space of the nuclei and one of the electrons. These data can be integrated over any desired coordinate to obtain ion energy and angular distributions as well as electron energy and angular distributions with respect to the photon polarization axis $\boldsymbol{\epsilon}$ and the internuclear axis. They can be compared with similar measurements we have made for helium, the corresponding atomic two-electron system.

So far only a few experimental studies have investigated this fundamental four-body problem. Kossmann *et al.* [4] and Dujardin *et al.* [6] measured the angular distribution of the two nuclei without detecting the electrons. Kossmann *et al.* [4] found close to threshold that the molecular breakup perpendicular to $\boldsymbol{\epsilon}$ is favored. The angular distributions of two equal energy electrons averaged over all molecular alignments have recently been found to be similar in structure to those for helium [1–3]. In the only theoretical study of differential cross sections for double photoionization of H_2, Le Rouzo [7] predicts the electron energy distribution to be significantly different from those known for double ionization of atomic targets [8,9]

We have used recoil ion momentum spectroscopy [10–12] to achieve simultaneous imaging of ion and electron momenta. A supersonic beam of D2 is intersected with the photon beam of beam line 9.0.1. at the Advanced Light Source at Lawrence Berkeley National Laboratory. All ions and electrons created in the overlap volume of the photon beam and the gas jet are guided by a static electric and a homogenous magnetic field [13] towards two position-sensitive channel-plate detectors. Both ions and one of the two electrons are detected. All time of flights and positions are recorded in list mode. From this information the vector momenta of the nuclei and the electron are calculated.

Figure 1(a) shows the momentum distribution of the fragment ions in the plane defined by $\boldsymbol{\epsilon}$ and the beam direction. The spectrum is integrated over all electron directions and energies. The fragments emerge most likely perpendicular to $\boldsymbol{\epsilon}$. We find a beta parameter for the ions of -0.6 ± 0.05, which is in reasonable agreement with the work of Kossmann *et al.* [4]. From 58.8 eV of total

 0031-9007/98/81(26)/5776(4)$15.00

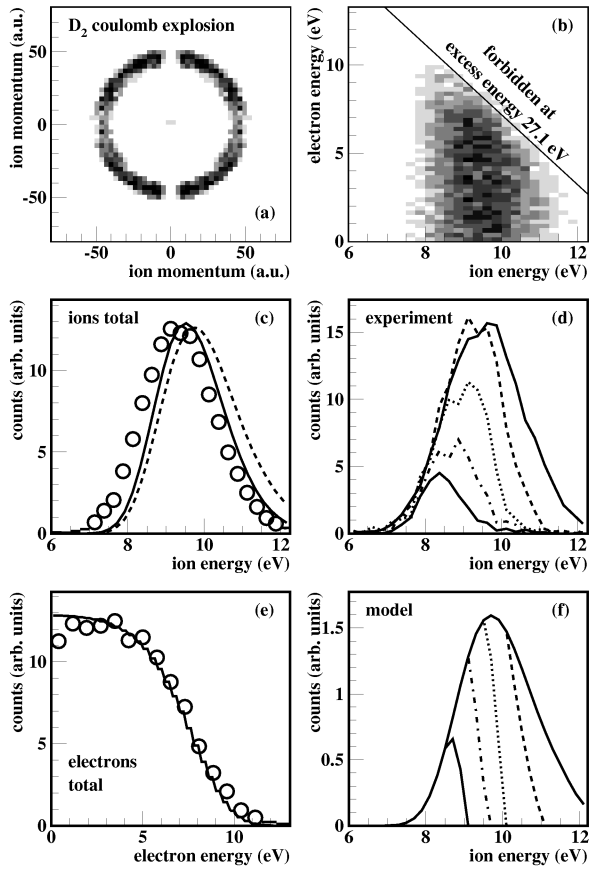

FIG. 1. (a) Relative momentum $\mathbf{k}_N$ distribution of the D^+ ions following double photoionization of D_2 by 58.8 eV linear polarized light. The electric field vector is horizontal, the light propagates in the vertical direction. The gap in the data is due to the finite pulse pair resolution of our detector. (b) Energy of one of the two electrons versus energy of one of the nuclei. The full line indicates the maximum available electron energy for a given ion energy. (c) Ion energy distribution integrated over all angles and electron energies. The full line shows the model discussed in the text, the dotted line the reflection approximation of the D_2 ground state. The remaining discrepancy between the full line and the data is within the uncertainty of our momentum calibration. (d) Ion energy distribution $d^2\sigma/dE_e dE_N$ for fixed electron energies (experiment). From right to left the electron energies are 0–4, 5–7, 7–8, 8–9, and 9–10 eV. (e) Electron energy distribution integrated over all ionic energies. The full line shows the prediction of the model discussed in the text. (f) Model prediction (see text); compare to (d).

photon energy, 27.1 eV can be shared as kinetic energy among the four fragments. For the nuclei we find a narrow energy distribution peaked around 9.4 eV [Fig. 1(c)]. This energy is slightly lower than what one would obtain from Coulomb repulsion if one instantaneously strips the two electrons from the D_2 ground state [dashed line in Fig. 1(c)]. The reason for this becomes obvious from Fig. 1(b), which shows the correlation between electronic and nuclear energy. The diagonal is the border given by energy conservation plus the fact that momentum conservation requires both ions to have (almost) identical energy (and opposite momenta). Thus the truncation in final state phase space apparently moves the ionic energies towards lower values, an effect already predicted by Le Rouzo [7]. The energy distribution of one of the two electrons, integrated over all nuclear energies and all electron and nuclear angles is shown in Fig. 1(e) [i.e., 1(e) is a projection of 1(b) onto the vertical axis]. Unlike atomic photoionization the electron energy distribution has no sharp upper threshold since it is integrated over all nuclear energies. The full line shows the prediction of a model suggested by LeRouzo [7]. This model invokes the axial recoil approximation [14] and thus takes the kinetic energy of the ions to be equal to their (repulsive) equilibrium-separation potential energy at the instant of double ionization. In addition, the model assumes no momentum is exchanged between the heavy and light fragments. The double ionization cross section at a given internuclear separation is assumed to scale according to the two-electron Wannier threshold law proportional $E^{1.056}$, where E is the energy shared by the two electrons. The form of the full line in Fig. 1(c) is not very sensitive, however, to the actual exponent. With the additional assumption of a flat energy distribution of one electron for fixed internuclear distance, analogous to helium double photoionization [8,9], the model predicts the electron energy distribution given by the full line in Fig. 1(e). The ion-energy distributions for fixed energy of one electron are found to be in good agreement with this simple model, too [Figs. 1(d) and 1(f)]. Thus we find a strong energy dependence between the ionic and the electronic motion. It can be understood, however, from a simple application of energy conservation and the three-body Wannier threshold law without dynamical coupling between electronic and ionic momenta, and thus does not indicate a deviation from the axial recoil approximation.

Angular distributions of the fragments prove to be much more sensitive probes of the details of the double ionization process than energy distributions. It has been pointed out by several authors [14–17] and recently demonstrated experimentally for various molecules [18–21] that the angular distribution of photoelectrons is a rich source of information if the molecular axis is fixed in space. Fixed alignment is expected to generally break the azimuthal symmetry of the system about $\boldsymbol{\epsilon}$. Elaborate electron-pair emission patterns, excluded for atomic photoionization by parity- and exchange-symmetry requirements, become possible. For single ionization of H_2, Kaplan and Markin [22] have predicted a wave effect in the electron angular distribution generated by the emission of the electron from two identical centers, analogous to two-slit interference (see also [23]). However, this effect is not expected to be particularly strong in the present experiment because of the relatively low photon energies used, resulting in de Broglie wavelengths of the emitted electrons several times larger than the initial internuclear separation.

We present electron angular distributions following full photofragmentation of D_2 for the two special alignments in which the molecular axis is parallel and perpendicular to $\boldsymbol{\epsilon}$. We use the spherical polar angle ϑ_e with respect

to $\boldsymbol{\epsilon}$ and the corresponding azimuthal angle ϕ_e between the planes defined by $\boldsymbol{\epsilon}$ and the molecular axis and $\boldsymbol{\epsilon}$ and the electron momentum vector. Figures 2(a)–2(c) show one-electron polar distributions for helium and for D_2 for parallel and perpendicular alignment. In all three cases the data are integrated over all azimuthal angles and all electron energies. The excess energy for the helium measurement was 7 eV, comparable to that for the D_2. All data have been measured with the same apparatus in the same beam time to reduce systematic errors. We estimate the remaining systematic error on the β parameter to be smaller than ± 0.1. Such errors would, however, influence all β parameters presented in this paper in the same way; relative to each other, the systematic errors are much smaller. While the helium data show an almost isotropic emission, the D_2 data in the parallel configuration show electrons emitted predominantly along $\boldsymbol{\epsilon}$. The D_2 data for parallel and perpendicular alignment differ significantly.

For the D_2 data in the perpendicular configuration, the azimuthal symmetry about $\boldsymbol{\epsilon}$ is broken by the alignment of the initial state. To search for a remnant of this alignment, we have plotted in Fig. 2(d) the azimuthal angular distribution of the electron in the plane perpendicular to $\boldsymbol{\epsilon}$. Here the molecular axis is fixed parallel to the horizontal axis of the plot. We find azimuthal symmetry around $\boldsymbol{\epsilon}$ even though the initial state is aligned.

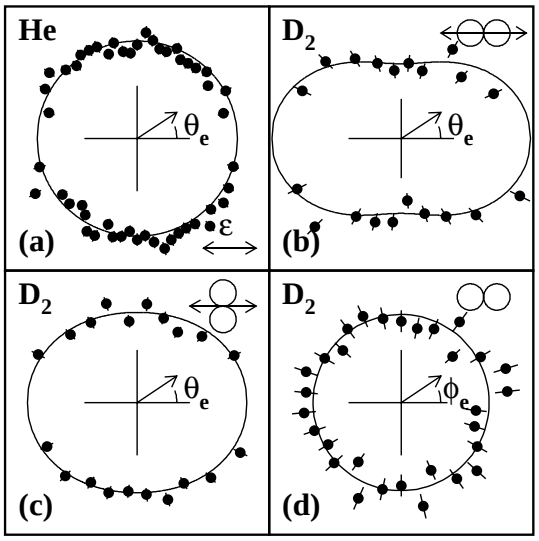

FIG. 2. Polar representation of the angular distribution of one of the two photoelectrons from double photoionization of helium at 7 eV excess energy and of D_2 also at about 7 eV excess energy [cf. Fig. 1(e)] (see text for definition of the angles). The data have been integrated over all electron energies. (a) $d\sigma/d\cos\vartheta_e$ for helium with $\boldsymbol{\epsilon}$ along the horizontal. The line shows a fit with $\beta_e = 0 \pm 0.04$. (b) $d\sigma/d\cos\vartheta_e$ for D_2 with $\boldsymbol{\epsilon}$ along the horizontal and the molecular axis held fixed parallel to $\boldsymbol{\epsilon}$. The line shows a fit with $\beta_e = 0.4 \pm 0.1$. (c) Similar to (b) but for alignment of the molecule perpendicular to $\boldsymbol{\epsilon}$. The data are integrated over all azimuthal angles. The line shows a fit with $\beta_e = 0.14 \pm 0.08$. (d) $d\sigma/d\phi_e$ for D_2 with $70° < \vartheta_e < 110°$ (90° is the plane of the paper). The molecule is held fixed perpendicular to $\boldsymbol{\epsilon}$, *which now points out of the paper*. The full line is a circle to guide the eye.

Because the double photoionization threshold lies some 50 eV above the molecular ground state and well above the *four-body* fragmentation threshold at 31.8 eV, we assume four-body saddle dynamics [24] to have little effect on the photofragmentation observed here. We introduce instead a simpler description based on the helium double ionization amplitude while recognizing excitation along the symmetry axes of the molecule. For a given ion-axis (relative-momentum) alignment $\mathbf{k}_N$ at the instant of photoexcitation, we thus derive [25] a molecular double ionization amplitude

$$f(\mathbf{k}_N) = g_\Pi(1,2)\,\boldsymbol{\epsilon}\cdot\hat{\mathbf{k}}_{e1} + g_\Pi(2,1)\,\boldsymbol{\epsilon}\cdot\hat{\mathbf{k}}_{e2} + \boldsymbol{\epsilon}\cdot\hat{\mathbf{k}}_N\big([g_\Sigma(1,2) - g_\Pi(1,2)]\hat{\mathbf{k}}_N\cdot\hat{\mathbf{k}}_{e1} + [g_\Sigma(2,1) - g_\Pi(2,1)]\hat{\mathbf{k}}_N\cdot\hat{\mathbf{k}}_{e2}\big), \tag{1}$$

where $\mathbf{k}_{ei=1,2}$ are the momenta of the ejected electrons and $g_\alpha(i,j)$ functions of the electron energies (E_i, E_j) and the mutual momentum angle $\theta_{12} = \cos^{-1}\hat{\mathbf{k}}_{e1}\cdot\hat{\mathbf{k}}_{e2}$. These functions are heliumlike amplitudes but generalized to include excitations parallel (g_Σ) and perpendicular (g_Π) to $\mathbf{k}_N$ [26]. Equation (1) reduces therefore to the helium excitation amplitude if $g_\Sigma = g_\Pi = g$. It also becomes a form identical with the helium amplitude when the photon electric field has a nonvanishing component along only one of the symmetry axes of the molecule: When $\boldsymbol{\epsilon} \parallel \mathbf{k}_N$, only parallel excitation occurs with $g = g_\Sigma$; when $\boldsymbol{\epsilon} \perp \mathbf{k}_N$, only perpendicular excitation occurs with $g = g_\Pi$. This description thus predicts azimuthal symmetry about $\boldsymbol{\epsilon}$ in both limits even though the symmetry is ostensibly broken in the latter limit in the initial state. This result is thus consistent with the observations presented in Fig. 2(d).

The square of the amplitude $f(\mathbf{k}_N)$ is readily integrated over, say, $\mathbf{k}_{e2}$ to define the single-electron distribution $d^2\sigma/d\hat{\mathbf{k}}_e d\hat{\mathbf{k}}_N$ we have measured here. The result for arbitrary ion-axis alignment $\mathbf{k}_N$ is more complicated than the familiar dipole excitation form, but reduces to $1 + \beta_e(\mathbf{k}_N)P_2(\boldsymbol{\epsilon}\cdot\hat{\mathbf{k}}_e)$ for pure parallel or perpendicular excitations, $\mathbf{k}_N \parallel \boldsymbol{\epsilon}$ or $\mathbf{k}_N \perp \boldsymbol{\epsilon}$. The solid lines through the data in Figs. 2(b)–2(d) are fits based on this formula integrated over all electron energies.

To check for an electron energy dependence of angular distribution, we have plotted β_e as a function of electron energy in Fig. 3. Integrating over all molecular alignment, the β_e for D_2 is slightly larger than for helium. Our data for helium are consistent with all data from other experiments taken at different photon energies and with several theoretical predictions [8,9,27,28]. Figure 3(b) shows β_e for parallel and perpendicular alignment of the D_2 molecule. The lines in Fig. 3(b) show fits from a more detailed parametrization of Eq. (1) based on a Wannier description of the electron-pair wave function (see [25]). The amplitudes $g_\Sigma(i,j)$ and $g_\Pi(i,j)$ were taken to be

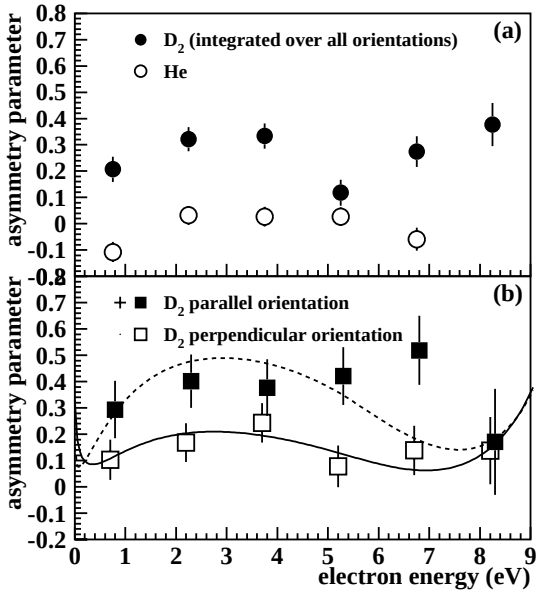

FIG. 3. β_e as a function of electron energy for double photoionization of helium at 7 eV excess energy and of D_2 also at about 7 eV excess energy [cf. Fig. 1(e)]. (a) D_2 integrated over all molecular alignments. (b) D_2 for molecular alignment parallel to $\boldsymbol{\epsilon}$ and perpendicular to $\boldsymbol{\epsilon}$. The lines in (b) show fits based on the heliumlike model for D_2 discussed in the text (see also [25]).

proportional to a Gaussian correlation function of $\pi - \theta_{12}$ familiar from studies of angular distributions in helium [1,2] with FWHM $\Delta\theta_{12}(\Sigma) = 135°$ and $\Delta\theta_{12}(\Pi) = 110°$, respectively. Although the fits in Fig. 3(b) are fairly rough, they require significantly larger FWHM than that obtained in helium $\Delta\theta_{12} \sim 91°$ (see [11], and references therein) or D_2 $\Delta\theta_{12} \sim 76°$ [1–3] at comparable photon energies. Hence, our angular asymmetry parameters β_e are large and within our simple model show puzzling inconsistency with previous findings.

Two possible explanations warrant further study. First, the derivation of Eq. (1) is based on the helium $^1S^e \rightarrow {}^1P^o$ *dipole* excitation amplitude and ignores higher electron-pair angular momentum components, which may modify the angular distributions and hence affect the angular asymmetry parameter. Second, the two-center interference effect in the electron emission mentioned earlier [22,23] produces a modulation of the angular distributions given by $\cos^2(\frac{1}{2}\,\mathbf{k}\cdot\mathbf{R}_N)$ [29]. Here R_N is the internuclear separation, while k could be the momentum of one electron [29] or the center of mass momentum of the electron pair, as has been argued recently by Berakdar *et al.* [30]. The difference in excess energy between 7 eV in the present work and 20 eV in the work of Refs. [1–3] can change this modulation as much as 50%, and it is an open question how this might influence the effective width of the Gaussian correlation function and thus β_e.

A conclusive solution of the seemingly simple problem of complete fragmentation of D_2 by a single photon remains illusive. We are currently performing experiments to measure the vector momenta of both nuclei and both electrons in coincidence. More structure in the angular distributions and a significant dependence with respect to the molecular axis might be expected at higher photon energies where contributions from higher angular momenta and interference effects may be more important.

The work was supported in part by BMBF, DFG, and the Division of Chemical Sciences, Office of Basic Energy Sciences, Offices of Energy Research, U.S. Dept. of Energy. We thank the staff of the Advanced Light Source for superb support during the beam time and A. Belkacem for lending of electronic equipment. One of us (H. B. R.) was supported by the Alexander von Humboldt Stiftung and another (R. D.) by the Habilitanden Programm der DFG. We thank our colleagues T. Reddish, V. Schmidt, J. Berakdar, and B. Joulakian for fruitful discussions.

*Email address: doerner@ikf.uni-frankfurt.de

[1] T. J. Reddish *et al.,* Phys. Rev. Lett. **79**, 2438 (1997).
[2] J. P. Wightman *et al.,* J. Phys. B **31**, 1753 (1998).
[3] N. Scherer *et al.,* J. Phys. B **31**, L817 (1998).
[4] H. Kossmann *et al.,* Phys. Rev. Lett. **63**, 2040 (1989).
[5] A. K. Edwards *et al.,* Phys. Rev. A **46**, 6970 (1992).
[6] G. Dujardin *et al.,* Phys. Rev. A **35**, 5012 (1987).
[7] H. LeRouzo, J. Phys. B **19**, L677 (1986); Phys. Rev. A **37**, 1512 (1988).
[8] R. Wehlitz *et al.,* Phys. Rev. Lett. **67**, 3764 (1991).
[9] D. Proulx and R. Shakeshaft, Phys. Rev. A **48**, R875 (1993).
[10] J. Ullrich *et al.,* J. Phys. B **30**, 2917 (1997), Topical Review.
[11] R. Dörner *et al.,* Phys. Rev. A **57**, 1074 (1998).
[12] R. Dörner *et al.,* Phys. Rev. Lett. **77**, 1024 (1996); **78**, 2031 (1997).
[13] R. Moshammer *et al.,* Nucl. Instrum. Methods Phys. Res., Sect. B **108**, 425 (1996).
[14] R. N. Zare, Mol. Photochem. **4**, 1 (1972).
[15] J. L. Dehmer and D. Dill, Phys. Rev. Lett. **35**, 213 (1975).
[16] D. Dill, J. Chem. Phys. **65**, 1130 (1976).
[17] D. Dill *et al.,* J. Chem. Phys. **65**, 3158 (1976).
[18] E. Shigemasa *et al.,* Phys. Rev. Lett. **74**, 359 (1995); **80**, 1622 (1998).
[19] N. Watanabe *et al.,* Phys. Rev. Lett. **78**, 4910 (1997).
[20] A. V. Golovin *et al.,* Phys. Rev. Lett. **79**, 4554 (1997).
[21] F. Heiser *et al.,* Phys. Rev. Lett. **79**, 2435 (1997).
[22] I. G. Kaplan and A. P. Markin, Sov. Phys. Dokl. **14**, 36 (1969).
[23] H. D. Cohen and U. Fano, Phys. Rev. **150**, 30 (1966).
[24] J. M. Feagin and R. D. Filipczyk, Phys. Rev. Lett. **64**, 384 (1990).
[25] J. M. Feagin, J. Phys. B **31**, L729 (1998).
[26] In the partial-wave analysis, Σ and Π designate the angular momentum projection quantum numbers $\mathbf{L}\cdot\hat{\mathbf{k}}_N = 0$ and 1, respectively, of the electron pair.
[27] F. Maulbetsch and J. S. Briggs, J. Phys. B **26**, 1679 (1993).
[28] H. P Bräuning *et al.,* J. Phys. B **30**, L649 (1997).
[29] M. Walter and J. S. Briggs, J. Phys. B (to be published).
[30] J. Berakdar *et al.,* Phys. Rev. Lett. **81**, 3535 (1998).